The role of the carrier gas flow in directed energy deposition

Available online at www.eccomasproceedia.org
Eccomas Proceedia SMART (2023) 1258-1269

ECCOMAS
Proceedia

X ECCOMAS Thematic Conference on Smart Structures and Materials
SMART 2023
D.A. Saravanos, A. Benjeddou, N. Chrysochoidis and T. Theodosiou (Eds)

THE ROLE OF THE CARRIER GAS FLOW IN THE DIRECTED ENERGY DEPOSITION PROCESS

A. N. PILAGATTI, E. ATZENI, L. IULIANO AND A. SALMI

Department of Management and Production Engineering (DIGEP)
Politecnico di Torino
Corso Duca degli Abruzzi 24, 10129 Torino, Italy
e-mail: adriano.pilagatti@polito.it, web page: www.polito.it

Abstract. Laser Powder-Directed Energy Deposition (LP-DED) is a metal Additive Manufacturing (AM) technique that can build, repair, and remanufacture metal components. The aim of this study was to investigate the physical contribution of the carrier gas flow in the building process. Several cubes were built with different levels of the carrier gas flow given the powder mass flow rate. The specimens were built on the same material. The final height of each cube was measured to estimate the influence of the carrier gas on the deposition. Based on the data analysis, it was possible to find out that the gas flow levels highly contribute, from the energetic point of view, to the melt pool process. Moreover, this study allowed improving the deposition efficiency in building cubes in AISI 316L steel with argon as the carrier gas.

Key words: Additive Manufacturing, Process Parameters, Design of Experiment, Directed Energy Deposition

1 INTRODUCTION

Laser Powder-Directed Energy Deposition (LP-DED) is a metal Additive Manufacturing (AM) technique that uses a laser to locally heat a substrate, creating a melt pool where new filler material in the form of powder is added. Metal powder particles are delivered to the melt pool through the deposition head by a carrier gas, such as argon or nitrogen. The deposition head is indeed a crucial component of the LP-DED system, comprising multiple elements including laser optics, powder-fed nozzles, shielding gas nozzles, and sensors [1]. Several deposition head configurations have been developed and are available for LP-DED. Initially, the lateral deposition head was developed as the first configuration, employing a single off-axis nozzle. However, this system has geometric limitations, which led to the development of two different coaxial configurations as alternatives. One configuration uses a discrete number of symmetrically positioned nozzles, while the other uses a coaxial conical nozzle. Among these options, the coaxial deposition head configuration has become the most widely used due to its greater precision and improved control over powder delivery [2]. Among powder metering and conveyance systems, the pneumatic ones are the most common in commercial DED machines.

Peer-review under responsibility of the organizing committee of SMART 2023.
doi: 10.7712/150123.9873.444102

One possible pneumatic powder handling method for LP-DED involves a disk, with holes at regular angles, that rotates against a fixed disk that features only one hole aligned with the inlet port of the laminated carrier gas. On the other side of the rotating disk, and aligned with the inlet port, is a conduit for powder transport. On the same side, the rotating disk is in continuous contact with the metallic powder that is released by gravity from the hopper into the metering system. When a hole of the rotating disk is aligned with the powder inlet, the hole of the stationary disks, and powder outlet, the Venturi effect causes the powder to be streamed through the outlet port. A stepper motor rotates the disk, and the combination of the size and number of holes, disk rotation speed, and carrier gas flow rate determine the powder mass flow rate [3].

The flow behaviors of the powder used in LP-DED significantly affect the interaction among the laser, powder, and melt pool, ultimately determining the track geometry and quality [4]. Experiments conducted by the authors on AISI 316L cubes revealed that a low carrier gas flow can cause the nominal height of a deposition not to be reached and thus compromise the construction of specimens. It is therefore important to deepen the knowledge on the effect of the carrier gas flow. In fact, although several mathematical models and experiments on the size and shape of single tracks have been conducted in the past, little attention has been paid to correctly characterize the effect of the carrier gas in the LP-DED and how this affects the layer height.

Shim et al. [5] conducted various experiments on the height growth between successive layers under different levels of power, powder feed rate, travel speed, shielding gas, and carrier gas. The depositions showed an almost linear increase in height with increasing levels of carrier gas. According to Dass and Moridi [6], carrier gas flow rate is a significant process parameter influencing the DED deposition. The combination of the carrier gas with other parameters and complex transport phenomena such as heat conduction, convection, and radiation makes it difficult to understand the effect of each process parameter on the overall DED process. One approach for evaluating this effect is to characterize the feeder system employing experiments or numerical simulations. For example, Bayat et al. [7] conducted both a multi-physics numerical simulation and a set of experiments on the maraging steel to investigate the effect of the carrier gas on the final deposition shape. Their findings revealed that the H/W ratio and wettability of the tracks could be manipulated by changing the carrier gas flow rate, thereby altering the powder particle speeds and production rate.

A computational framework was proposed by Yao et al. [8] to study energy distribution during laser powder-directed energy deposition. The results showed that increased gas flow rates led to increased laser energy distribution and decreased average temperature rise of powder particles. Stavropoulos et al. [9] optimized the equipment for increasing the deposition rate of a DED machine using an analytical process model and CFD simulation results. Jinoop et al. [10] conducted a systematic study to develop the process window and an empirical model for the track width of IN718 thin walls using DED. This study showed that the fabricated thin walls were defect-free with fine dendritic microstructure, and post-heat treatment resulted in reduced surface residual stress and improved ductility and energy storage capacity. Woo et al. [11] proposed a corner scanning speed control method to reduce excessive deposition at rectangular corners during DED fabrication. The proposed method is based on bead geometry prediction

and was successfully implemented to fabricate a rectangular box. The study conducted by Shim et al. [12] found that substrate preheating with an induction heater effectively reduced crack susceptibility during the metal deposition of HSS M4 powder. The study analyzed the microstructure evolution, microhardness, melting pool position, and tensile behavior of deposited specimens and confirmed the positive effect of preheating.

Another possible approach, alternative to numerical simulation, to solve process and manufacture problems is the data-driven method. The latter involves analyzing large data sets to identify patterns, relationships, and trends. It can be used to develop statistical models that can predict the behavior of a system or process based on historical data. The advantage of this approach is the independence from a detailed knowledge of the underlying physics of the system, making it suitable for complex systems where analytical modelling can be challenging. However, this method requires large amounts of high-quality data to be collected and processed, which may be time-consuming and expensive [13, 14].

The purpose of this paper is to present a black box approach to investigate the effect of carrier gas levels on the growth of cubic specimens in AISI 316L produced by LP-DED on a substrate of same material and to provide a set of criteria for selecting the appropriate gas flow rate. In details, firstly an equation was derived to calculate the powder mass flow rate required to meet the volume to be deposited with a given input energy. The powder mass flow rate is governed by the carrier gas flow and the height of depositions was correlated to the levels of carrier gas using a design of experiment (DoE), developed on the bases of the potential causes of failure identified through t-test analysis. The experiment results were analyzed using a statistical method to identify significant factors. The response behavior was obtained by the Response Surface Methodology (RSM), identifying the right combinations of levels and factors to be able to build the specimens correctly in terms of height. The results provide valuable insights into the influence of the carrier gas on the deposition process.

2 MATERIAL AND METHODS

The DED system utilized in this study is the Laserdyne 430 by Prima Additive (Torino, Italy) equipped with the CF 1000 fibre laser by Convergent Photonics (Torino, Italy) with a maximum power of 1 kW and a wavelength of 1075(3) nm*. In the existing configuration, the laser spot diameter, D, equals 2.00(1) mm. The powder feeding system is an Optomec (Albuquerque, NM, USA) system, which features a rotating disk in combination with a gravity hopper that utilizes argon under fixed pressure of 5.0(3) bar. The deposition head has four equi-spaced discrete nozzles converging at an 8 mm standoff distance. The feedstock material is a commercially available gas-atomized pre-alloyed MetcoAdd 316L-D austenitic stainless steel powder by Oerlikon (Freienbach, Switzerland). It has a unimodal and Gaussian particle size distribution with d_{10} = 49.2 µm, d_{50} = 60.9 µm, and d_{90} = 74.6 µm. Moreover, the powder exhibits a Hall funnel flow rate of of 15.26(8) s, and the Carr's compressibility index of 8.3%.

* All the uncertainties in parentheses are expressed as recommended by the GUM [15], and they have been calculated assuming Type B errors with a rectangular distribution [16].

The need for the current study arose from the observation of a growth defect that emerged during a related experiment and was attributed to the carrier gas. Thus, in the following, firstly the antecedent experience is described, followed by the main focus of this work, which is to provide a detailed analysis of the carrier gas and its impact on the height of the depositions.

2.1 Antecedent experience

An antecedent experience was carried out to characterize the amount of powder that should be spread on the laser spot compared to the geometric parameters of the track to be built. To this aim, a dimensionless parameters, R, was introduced. R is the ratio of the volumetric flow rate of powder coming from the deposition head, Q_p, to the track volume to be built in a unit time, Q_t. The R coefficient is defined as follows:

$$R = \frac{Q_p}{Q_t} = \frac{Q_p}{\Delta Z v D \rho_p} \tag{1}$$

where Q_p is the powder mass flow rate expressed in g/min and ρ_p is the powder density in g/mm^3. The Q_t can be roughly estimated as the product of track height ΔZ (defined by the Z-displacement of the deposition head at each new layer), the laser spot diameter, D, and the travel speed, v. All parameters units are chosen in such a way as to be consistent and oriented to obtain Q_p in the desired units.

In an ideal scenario without powder losses, R should be equal to 1. The previous equation was then modified by the authors to include other effects. Specifically, to account for the surplus of powder used in the process that does not contribute to track generation, a new dimensionless coefficient factor named k was introduced. Moreover, the overlap efficiency, O_e, was included in the equation to consider the overlap of two consecutive tracks. Overlap values of 75 %, 50 %, 33.3 % or 0 % imply a multiplication factor of 4, 3, 2 or 1, respectively, of the number of tracks required to complete a given layer width. Finally, the Q_p equations can be expressed by:

$$\begin{cases} Q_p = k[R\Delta Z v D \rho_p (100 - O_e)] \\ Q_p = f(Q_{Ar}, \omega) \end{cases} \tag{2}$$

as indicated by the second relationship in Eq. 2, in the powder feeder system used in this work, Q_p is controlled by two parameters, namely the carrier gas flow rate, Q_{Ar}, expressed in L/min and the rotation of the disk, ω, expressed in rpm.

In the experiments, a single-replicate 2^{k-p} design with four quantitative factors (E, ΔZ, k, and Q_{Ar}), one qualitative factor (O_e), and p blocks was adopted. This type of design is often used in screening experiments when many factors are considered. Good practice in such cases is aggressively spreading out the factor levels and using center points to estimate the experimental error [17]. Moreover, the interactions were not considered by exploiting the sparsity of effects principle to improve the error estimation. Prismatic specimens with dimensions of $10 \times 10 \times 15.6\,\text{mm}^3$ were built on a substrate measuring $120 \times 120 \times 7\,\text{mm}^3$. The values of the factor levels used are shown in Table 1. For the current experiment, ω values were determined

Table 1: Process variables values and center points used in the planned experimentation

Process variable	Values	Center point
E (J/mm^2)	46 – 60	53
ΔZ (mm)	0.4 – 0.6	0.5
Q_{Ar} (L/min)	2 – 6	4
k	1.00 – 1.50	1.25
O_e (%)	0 – 50	/
R	1	1

from system characterization to establish Q_p values as a function of R (set to unity) and k with varying Q_{Ar} levels solving the Q_p equation system. As a result, ω is a dependent variable of the system of equations, obtained through a straightforward calculation with Q_{Ar} and k inputs. The authors derived the function linking Q_p to Q_{Ar} and ω through an experiment to obtain the system response surface. Moreover, it should be noted that specific energy values can be obtained for infinite combinations of power and v. Given that the maximum power of the system used is 1 kW and that for equipment working with heat sources, the risk of damage increases with the operating temperature, in this work, the operating value of power was set to 80 % of the maximum as suggested by Cengel and Ghajar [18]. Consequently, v was varied to obtain the desired energies.

Out of ten specimens, already on visual inspection four showed inadequate growth, reaching approximately half the expected height. To measure the distance between the substrate and the top of the specimens, a gauge system was mounted on a custom-designed gauge marker and used to acquire the position of four points on the substrate and five points on the top of the

Table 2: First trial height values

Std. Order	Run Order	Position	E (J/mm^2)	ΔZ (mm)	Q_{Ar} (L/min)	O_e (%)	k	Height (mm)	Height (%)
1	**10**	**5**	**46**	**0.4**	**2**	**0**	**1**	**6.7**	**42.9**
2	**4**	**10**	**60**	**0.6**	**2**	**0**	**1**	**6.9**	**44.2**
3	3	7	60	0.4	6	50	1	15.8	101.3
4	8	2	46	0.6	6	50	1	15.6	100.0
5	2	1	60	0.4	6	0	1.5	17.3	110.9
6	6	9	46	0.6	6	0	1.5	16.1	103.2
7	**9**	**6**	**46**	**0.4**	**2**	**50**	**1.5**	**8.8**	**56.4**
8	**5**	**8**	**60**	**0.6**	**2**	**50**	**1.5**	**8.3**	**53.2**
9	1	3	53	0.5	4	0	1.25	12.6	80.8
10	7	4	53	0.5	4	50	1.25	13.1	83.7

specimens, to compensate both the substrate distortions and geometric up-skin defects. The surfaces were interpolated, and the height for each specimen was obtained by taking the mean distance between the two surfaces. The Table 2 data displays both the actual height values of the samples as well as the percentage growth in height relative to the nominal values. The common factor of failed specimens was identified in the low Q_{Ar} level (2 L/min).

The experiment was terminated, and a second test trial was conducted on the opposite face of the same substrate, improving the precision of the experiment by avoiding the blocking nuisance effect that could be caused by the difference between two substrates [19]. Moreover, to conform with the other two fundamental principles of industrial experiments, i.e., randomization and replication, the standard order and position of the specimens on the substrate were maintained, while the run order was changed randomly. This way, it is easier to observe the differences between the specimens due to their positions while complying with the principle of randomization.

Due to the limited resources and costs of this experiment, only four replications were available for both low gas levels. The objective was to determine whether there was an improvement in response by increasing the low and intermediate Q_{Ar} level from 2 and 4 to 4 and 5 L/min. The results showed an improvement in response in all the increased low Q_{Ar} levels (Table 3 and Figure 1).

A Two-Sample T-Test with a 95 % confidence interval (CI) between the first and the second run was performed on specimen height at low Q_{Ar} levels, assuming equal variances between treatments. The statistical analysis showed a significant difference between the two levels of carrier gas, as the p-value obtained was less than 0.01 %. Therefore, the null hypothesis was rejected, and we concluded that the increase in the level of carrier gas leads to an improvement in the height of the specimens. As Gibson et al. [1] mentioned, *"The kinetic energy of powder particles being fed into the melt pool is greater than the effect of gravity on these powders during flight"* and this aspect was related to the observed deposition failures. In fact, it can also be

Table 3: Second trial height values

Std. Order	Run Order	Position	E (J/mm^2)	ΔZ (mm)	Q_{Ar} (L/min)	O_e (%)	k	Height (mm)	Height (%)
1	**3**	**5**	**46**	**0.4**	**4**	**0**	**1**	**13.1**	**84.0**
2	**6**	**10**	**60**	**0.6**	**4**	**0**	**1**	**12.5**	**79.8**
3	8	7	60	0.4	6	50	1	16.4	105.1
4	4	2	46	0.6	6	50	1	15.8	101.0
5	2	1	60	0.4	6	0	1.5	17.3	110.6
6	5	9	46	0.6	6	0	1.5	16.4	105.1
7	**1**	**6**	**46**	**0.4**	**4**	**50**	**1.5**	**15.8**	**101.0**
8	**10**	**8**	**60**	**0.6**	**4**	**50**	**1.5**	**14.8**	**94.6**
9	7	3	53	0.5	4	0	1.25	15.3	97.8
10	9	4	53	0.5	4	50	1.25	13.1	97.4

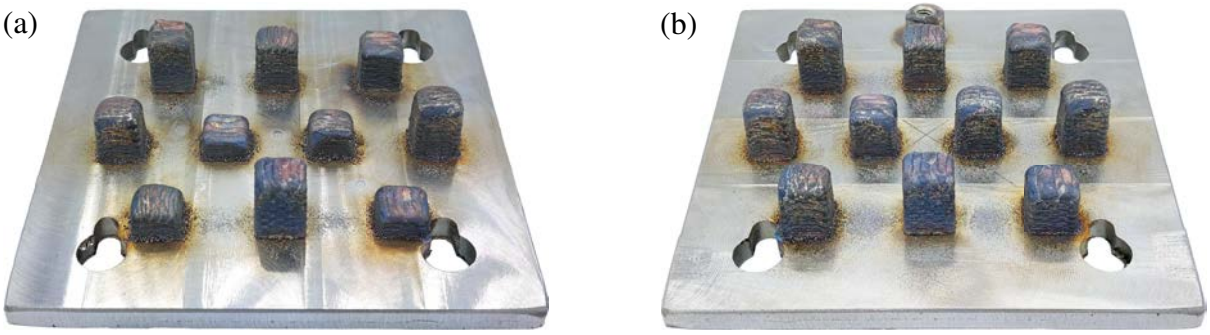

Figure 1: Comparison between (a) First trial and (b) Second trial

asserted that the speed of in-flight powder is affected by the Q_{Ar} rate, and for low values of the latter, the correct energy level required by the melt pool is not reached. This significant result indicates the need for a new experiment to be carried out in which the Q_{Ar} and k will be optimized to achieve the correct height of the specimens, which is the core of this paper. The physical phenomenon will not be explored in this work and will be addressed through a black-box approach.

2.2 New trials

Since kinetic energy is related to powder velocity through an exponential function, the 3^2 full factorial design has been selected, capable of modelling such non-linearities between factors and response. The number of replications should be calculated based on a pilot study, as suggested by Mathews [20], and contextualized with the objective of the effect size that needs to be predicted. However, three replications were selected to fully utilize the plate due to the availability of only one AISI 316L substrate of $250 \times 250 \times 10\,\text{mm}^3$ dimensions. A total of 27 cubic specimens measuring $10 \times 10 \times 10\,\text{mm}^3$ were then built on the same substrate. The process parameters utilized in this study were selected as the center point of the two previous tests (see Table 1), except O_e, which was chosen as 50 % because it is treated as a qualitative rather than quantitative factor. The two input variables related to height, namely Q_{Ar} and k, were kept at three levels, as detailed in Table 4.

Moreover, it is worth mentioning that while the temperature and humidity levels within the construction chamber are not controllable, they can be monitored. The experiment was thus conducted on a single day, and the boundary conditions (covariates) were monitored. These were

Table 4: Process variables values used in the planned experimentation

Process variable	Values
Q_{Ar} (L/min)	5 – 6 – 7
k	1.00 – 1.25 – 1.50

acquired through an *ad hoc* designed system, which used a simple moving average algorithm to provide the mean values of temperature and absolute humidity recorded in the construction chamber during the deposition process. The heights of the specimens were then measured as for the previous trials using a gauge system mounted on a custom-designed gauge marker. Finally, an ANCOVA analysis of measured heights as a percentage of the target was performed to identify the active factors in the process and apply the RSM to obtain and study the response surface and locate the target, where applicable.

3 RESULTS AND DISCUSSION

This experiment aimed to identify the optimal combination of Q_{Ar} and k factors to achieve the desired height of the deposited samples while holding all other process parameters constant. The impact of Q_{Ar} was observed in the two previous trials, indicating its significance in the process. A preliminary analysis to verify if the normality assumption for the regression model is justified was performed by plotting the response on a normal probability plot (NPP), as shown in Figure 2a. Then, after obtaining the model, the standardized residuals were analyzed. The latter did not exhibit any non-normal behavior, which was further confirmed by the Anderson-Darling test with a p-value of 50 %, surpassing the chosen significance level of 5 %. The normality of the standardized residuals suggests that the underlying assumptions of the linear regression model are met, indicating that the model is of good quality. Moreover, the regression model resulted in a standard deviation for residuals (S) of 7.3 and an $R^2(adj)$ of 68.75 %, indicating the proportion of total variability in the data explained by the model adjusted for the number of predictors in the model. Although these values are almost satisfactory, the model can be improved by conducting other experiments to increase the number of replications. The Table 5 indicates that only the Q_{Ar} factor significantly contributes to the chosen significance level.

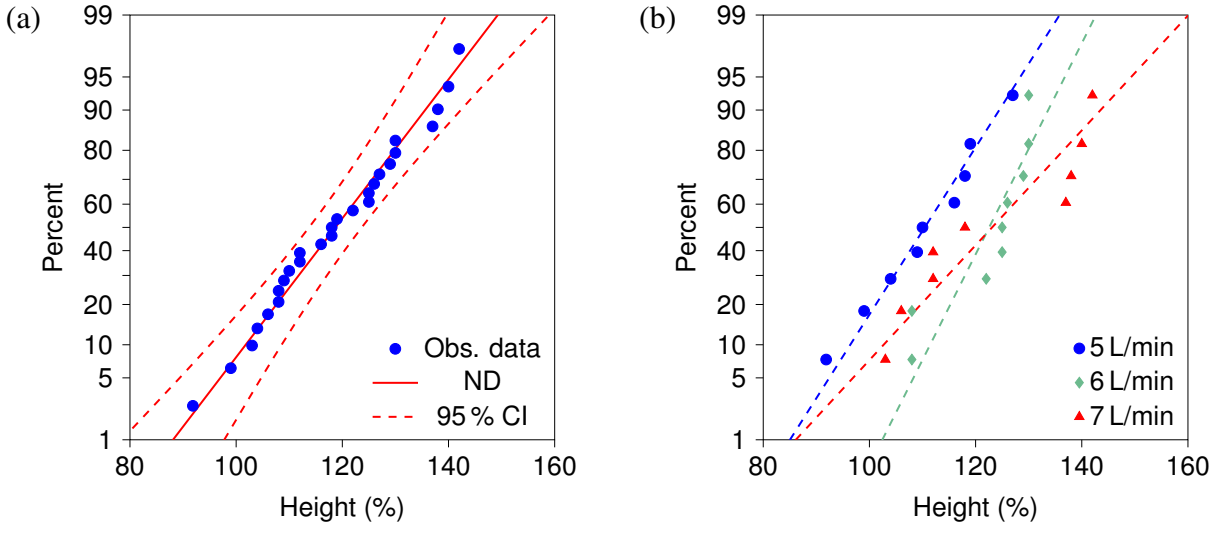

Figure 2: Normal probability plots (a) for the height of the specimens and (b) for height respect Q_{Ar} levels (Johnson's method)

Table 5: ANCOVA for height (%)

Source	df	Contribution (%)	Adj SS	Adj MS	F	p-value (%)
Model	10	80.77	3640.90	364.09	6.72	≤0.1
Covariates	2	64.54	1745.49	872.75	16.11	≤0.1
Temperature (°C)	1	63.84	67.25	67.25	1.24	28.2
Humidity (g/m^3)	1	0.70	41.59	41.59	0.77	39.4
Linear	4	14.72	651.19	162.80	3.01	5
Q_{Ar}	2	13.94	587.40	293.70	5.42	1.6
k	2	0.78	30.93	15.47	0.29	75.5
2-Way Interactions	4	1.15	68.14	17.03	0.31	86.4
$Q_{Ar} \cdot k$	4	1.15	68.14	17.03	0.31	86.4
Error	16	19.23	866.76	54.17		
Total	26	100				

However, the data collected suggest that the k factor and the interaction do not significantly impact the response.

In this case, the factorial plot is not informative, as only the Q_{Ar} factor is significant. As for the first two tests, increasing the Q_{Ar} results in an increase in the height of the specimens. However, by applying the Johnson plot method and visualizing the results on the NPP, a better understanding of the responses can be obtained, as the levels of the individual factors vary [21]. Specifically, when applying this method to the Q_{Ar} factor, it can be observed that the distribution is not normal for high Q_{Ar} level, as evidenced by two distinct clusters visible with red triangles (7 L/min) in Figure 2b. This non-normal behavior, combined with greater data dispersion, leads to instability in the process and, consequently, in the response.

In the following analysis step, the RSM was applied to model the relationship between the process parameters and the response. A full quadratic model was used, and a standard stepwise regression was performed to obtain a model containing only significant factors. Alpha-to-Enter and Alpha-to-Remove were set to 10 %, allowing for the inclusion of terms close to the significance level of 5 %. This approach enabled the identification of the most critical factors and their interactions, which were then used to determine the optimal process settings for achieving the desired response. The result is a linear regression equation, for the described method, with only the term Q_{Ar}, based on the selected levels for this factor. This finding is in agreement with the results obtained from the ANCOVA analysis. Finally, the equation in coded terms is:

$$\text{Height}\,(\%) = 118.6 + 6.34 \cdot Q_{Ar} \tag{3}$$

It is worth noting that only the linear term is significant at the chosen significance level (5 %). Moreover, the p-value of the lack-of-fit test is higher than the considered alpha, indicating no evidence that the model does not explain the data.

4 CONCLUSIONS

In this study, the aim was to find the correct combinations of Q_{Ar} and k to achieve the desired height of the deposited samples while keeping all other process parameters fixed. Previous studies needed to improve and simplify the methodology used. Therefore, in this study, a full factorial design of type 3^k was adopted, which allowed for the modelling of the non-linearity between factors and response. A commercially available gas-atomized 316L stainless steel powder was used as the starting material. The data were analyzed using ANCOVA, Johnson plot, and stepwise for RSM. The results showed that only the term Q_{Ar} was significant, and its instability at high levels led to unstable behavior in the process and response. The results suggest avoiding high Q_{Ar} levels for the powder, gas, and system under consideration. At the same time, low Q_{Ar} levels should also be avoided due to insufficient energy and limited sample fabrication. In addition, high Q_{Ar} levels should be avoided as they may result in an unstable process, requiring further investigation in future studies.

The present work contributes to the research in this field by providing a novel approach to achieve the desired height of the deposited samples in the DED system. The achievement in this work is the development of a method that considers the non-linear relationship between factors and response. The implications of this achievement are significant, as it can be applied in a wide range of DED manufacturing processes.

However, the limitations of this study should be addressed in future research. Specifically, the small sample size and the fact that only one substrate was available for the experiment should be considered. Future research should also explore the relationship between the temperature and humidity inside the construction chamber for more comprehensive and different ranges. In conclusion, the present study provides a foundation for further research in this field. Future work should refine the method and expand its application to other materials and systems.

ACKNOWLEDGEMENTS

The authors would like to sincerely thank the Interdepartmental Center for Integrated Additive Manufacturing (IAM@PoliTo) at the Politecnico di Torino, Torino, Italy, for providing the necessary machinery, materials, and technical support. Special thanks go to Giovanni Marchiandi and Matteo Perrone for their valuable assistance throughout the project. The authors also wish to thank Mattia Glorioso for his valuable contributions for the BCs monitoring system.

REFERENCES

[1] I. Gibson, D. Rosen, and B. Stucker, *Additive manufacturing technologies: 3D printing, rapid prototyping, and direct digital manufacturing*, 2nd ed. New York, NY: Springer, 2015.

[2] G. Piscopo, E. Atzeni, A. Saboori, and A. Salmi, "An overview of the process mechanisms in the laser powder directed energy deposition," *Applied Sciences*, vol. 13, no. 1, 2023.

[3] A. Singh, S. Kapil, and M. Das, "A comprehensive review of the methods and mechanisms

for powder feedstock handling in directed energy deposition," *Additive Manufacturing*, vol. 35, p. 101388, 2020.

[4] A. J. Pinkerton, "Advances in the modeling of laser direct metal deposition," *Journal of Laser Applications*, vol. 27, no. S1, p. S15001, 2015.

[5] D.-S. Shim, G.-Y. Baek, J.-S. Seo, G.-Y. Shin, K.-P. Kim, and K.-Y. Lee, "Effect of layer thickness setting on deposition characteristics in direct energy deposition (ded) process," *Optics & Laser Technology*, vol. 86, pp. 69–78, 2016.

[6] A. Dass and A. Moridi, "State of the art in directed energy deposition: From additive manufacturing to materials design," *Coatings*, vol. 9, no. 7, p. 418, 2019.

[7] M. Bayat, V. K. Nadimpalli, F. G. Biondani, S. Jafarzadeh, J. Thorborg, N. S. Tiedje, G. Bissacco, D. B. Pedersen, and J. H. Hattel, "On the role of the powder stream on the heat and fluid flow conditions during directed energy deposition of maraging steel—multiphysics modeling and experimental validation," *Additive Manufacturing*, vol. 43, p. 102021, 2021.

[8] X. X. Yao, J. Y. Li, Y. F. Wang, X. Gao, T. Li, and Z. Zhang, "Experimental and numerical studies of nozzle effect on powder flow behaviors in directed energy deposition additive manufacturing," *International Journal of Mechanical Sciences*, vol. 210, p. 106740, 2021.

[9] P. Stavropoulos, H. Bikas, and T. Bekiaris, "A powder delivery system for large-scale ded machines," in *Procedia CIRP*, vol. 109, 2022, pp. 617–622, export Date: Feb. 20, 2023.

[10] A. N. Jinoop, C. P. Paul, S. K. Mishra, and K. S. Bindra, "Laser additive manufacturing using directed energy deposition of inconel-718 wall structures with tailored characteristics," *Vacuum*, vol. 166, pp. 270–278, 2019.

[11] Y. Y. Woo, S. W. Han, I. Y. Oh, Y. H. Moon, and W. Ha, "Control of directed energy deposition process to obtain equal-height rectangular corner," *International Journal of Precision Engineering and Manufacturing*, vol. 20, no. 12, pp. 2129–2139, 2019, export Date: Feb. 20, 2023.

[12] D.-S. Shim, G.-Y. Baek, and E.-M. Lee, "Effect of substrate preheating by induction heater on direct energy deposition of aisi m4 powder," *Materials Science and Engineering: A*, vol. 682, pp. 550–562, 2017.

[13] P. Rey, C. Prieto, C. González, K. Tzimanis, T. Souflas, P. Stavropoulos, J. S. Rathore, V. Bergeaud, C. Vienne, and P. Bredif, "Data analysis to assess part quality in ded-lb/m based on in-situ process monitoring," in *Procedia CIRP*, vol. 111, 2023, pp. 345–350.

[14] P. Stavropoulos, H. Bikas, K. Sabatakakis, C. Theoharatos, and S. Grossi, "Quality assurance of battery laser welding: A data-driven approach," *Procedia CIRP*, vol. 111, pp. 784–789, 2022.

[15] Joint Committee for Guides in Metrology, "Evaluation of measurement data — guide to the expression of uncertainty in measurement," https://www.bipm.org/documents/20126/2071204/JCGM_100_2008_E.pdf/cb0ef43f-baa5-11cf-3f85-4dcd86f77bd6, 2008, accessed: 2023-05-05.

[16] E. O. Doebelin, *Measurement Systems: Application and Design*. New York, NY: McGraw-Hill, 2004.

[17] D. C. Montgomery, *Design and Analysis of Experiments*, 9th ed. New York, NY: Wiley, 2022.

[18] Y. A. Cengel and A. Ghajar, *Heat and Mass Transfer: Fundamentals and applications*, 5th ed. New York, NY: McGraw-Hill Education, 2015.

[19] D. R. Cox and N. Reid, *The Theory of the Design of Experiments*. New York, NY: Chapman and Hall/CRC, 2000.

[20] P. Mathews, *Sample size calculations: Practical methods for engineers and scientists*. Houston, TX: Mathews Malnar and Bailey, 2010.

[21] J. Neter, M. H. Kutner, C. J. Nachtsheim, and W. Wasserman, *Applied Linear Statistical Models*. New York, NY: McGraw-Hill, 1996.